IEEE Photonics Journal
An IEEE Photonics Society Publication

Open Access

A Reconfigurable High-Order UWB Signal Generation Scheme Using RSOA-MZI Structure

Volume 6, Number 2, April 2014

Hanlin Feng
Mable P. Fok
Shilin Xiao
Jia Ge
Qi Zhou
Mary Locke
Ryan Toole
Weisheng Hu

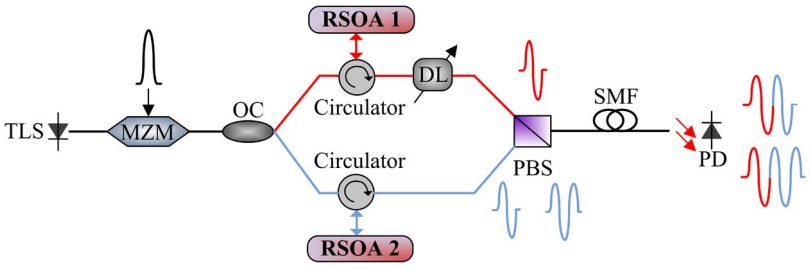

DOI: 10.1109/JPHOT.2014.2306832
1943-0655

A Reconfigurable High-Order UWB Signal Generation Scheme Using RSOA-MZI Structure

Hanlin Feng,[1,2] Mable P. Fok,[2] Shilin Xiao,[1] Jia Ge,[2] Qi Zhou,[2] Mary Locke,[2] Ryan Toole,[2] and Weisheng Hu[1]

[1]State Key Laboratory of Advanced Optical Communication Systems and Networks, Shanghai Jiao Tong University, Shanghai 200240, China
[2]Lightwave and Microwave Photonic Laboratory, College of Engineering, University of Georgia, Athens, GA 30602 USA

DOI: 10.1109/JPHOT.2014.2306832

Manuscript received January 8, 2014; revised February 1, 2014; accepted February 4, 2014. Date of publication February 21, 2014; date of current version February 28, 2014. The work was supported in part by the National Natural Science Foundation of China under Grants 61271216, 61221001, 61090393, and 60972032; by the National "973" Project of China under Grants 2010CB328205, 2010CB328204, and 2012CB315602; by the National "863" Hi-tech Project of China; and by the China Scholarship Council under Grant [2013]3009. Corresponding author: H. Feng (e-mail: fenghanlin@sjtu.edu.cn).

Abstract: We propose and experimentally demonstrate a reflective semiconductor optical amplifier (RSOA)-based Mach–Zehnder interferometer structure for generating high-order ultrawideband (UWB) signals. First, low-order UWB signals are generated by controlling the bias current of the RSOA. To convert the generated low-order UWB signals to high-order UWB signals, the polarization overlaying technique is used in an interferometer structure. The generated high-order UWB signals well satisfy Federal Communications Commission spectral regulations, and the interference with GPS band at 1.57542 GHz is suppressed.

Index Terms: Microwave photonics, fiber optics, ultrawideband.

1. Introduction

Ultra-wideband (UWB) signals are considered as the most promising schemes for next generation wireless communication systems. This type of signal is applicable for short range wireless communication systems, such as indoor wireless communication networks, intra-vehicle networks and wireless sensor networks. According to the limits set by the Federal Communications Commission (FCC), the power spectral density of a UWB signal is limited to below −41.3 dBm/MHz, and is ranged from 3.1 GHz to 10.6 GHz. A 10-dB spectral width is required to exceed 500 MHz with a corresponding fractional bandwidth that is 20% larger than the center frequency. UWB signals that meet these requirements are free for unlicensed use. Unfortunately, with such a low power density, the communication range of UWB signals is constrained to several meters [1], [2]. However, with photonic generation of UWB signals and transmission through an optical fiber, the transmission distance of UWB signals is greatly increased.

Photonic UWB signals have preferable characteristics of electro-magnetic compatibility, high data rate, and low transmission loss, and they are flexibly reconfigurable. Currently, approaches for the photonic generation of UWB signals can be categorized into Mach–Zehnder modulator (MZM) transmission curve utilization [3], phase modulation to intensity modulation conversion [4]–[6],

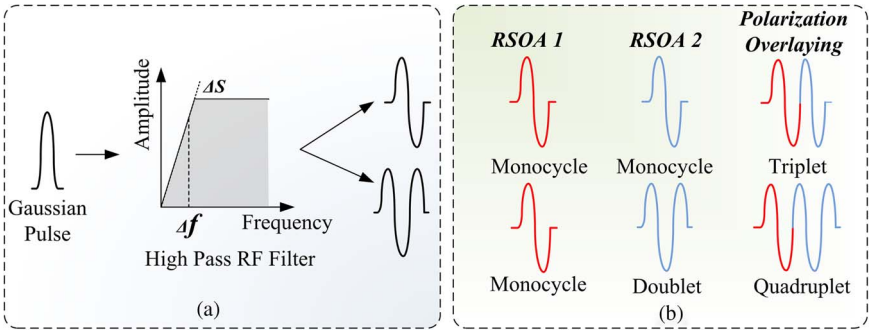

Fig. 1. Principle of high order UWB signals generation based on RSOA-MZI structure. (a) High-pass RF filter. (b) Polarization overlaying.

microwave photonic filtering (MPF) [7], [8], and utilizing nonlinear effects such as cross gain modulation (XGM) [9], cross phase modulation (XPM) [10], [11], and four wave mixing (FWM) [12]. In most of these schemes, low-order derivative UWB signals (i.e., first- and second- order) are easily generated. In practical application, interference between UWB systems and other wireless communications should be considered, particularly the jamming problem within GPS band [13], [14]. Low-order UWB signals have a strong power spectrum density (PSD) between 0 GHz and 2 GHz, which mismatches the power dip required between 0.96 GHz and 1.61 GHz, and lead to severe interference. On the contrary, high-order UWB signals have low PSD in the low frequency region, which essentially reduces the interference with a GPS system. As the UWB order increases, interference between UWB signals and other wireless communication signals decrease. Thus, intensive researches have been focused on the generation of high-order UWB signals (i.e., third order or above). Examples include the use of asymmetric MZI (AMZI) structure with polarization maintaining fiber and polarizer [15], N tap microwave photonic filter [8], overlaying complementary doublet pulses generated by polarization modulation and orthogonal polarization splitting and combining [16].

In this paper, we design and experimentally demonstrate the generation of a reconfigurable high-order UWB signals based on the use of reflective semiconductor optical amplifier in a Mach–Zehnder interferometer (RSOA-MZI) structure. Our approach is compact, simple, and requires only a single wavelength. UWB signal from first-order to forth-order is generated from the scheme. RSOA is a colorless and cost-effective device that is commonly used in optical access networks [17], [18]. RSOA has been used to generate low-order UWB signals. First-order UWB signal (monocycle) is generated based on gain saturation effect in RSOA [19], while the second-order UWB signal (doublet) is generated based on cascaded turbo-switch RSOA structure [20]. Additionally, by combining the gain switching effect with a balanced detector, third-order UWB signal (triplet) is achieved [21]. In our scheme, we experimentally obtained reconfigurable third- and fourth-order UWB signals (triplet and quadruplet) by overlapping low-order UWB signals with orthogonal polarization states. In our approach, low-order UWB signals are generated through the controllable gain saturation effect in RSOA, while reconfigurable high-order UWB signals are generated based on the use of polarization overlaying low-order UWB signals in a RSOA-MZI structure. The generated reconfigurable high-order UWB signals are completely complied with FCC regulations. Moreover, due to the single wavelength operation in our scheme, the generated high order UWB signals are tolerance to fiber dispersion, transmission through 10-km of fiber is experimentally demonstrated.

2. Principle and Experimental Setup

The principle of generating high-order UWB signals by using RSOA-MZI structure is shown in Fig. 1. In Fig. 1(a), the RSOA is regarded as a high-pass radio frequency (RF) filter with cut-off frequency Δf. Through adjusting the cut-off frequency of this high-pass filter, different-orders

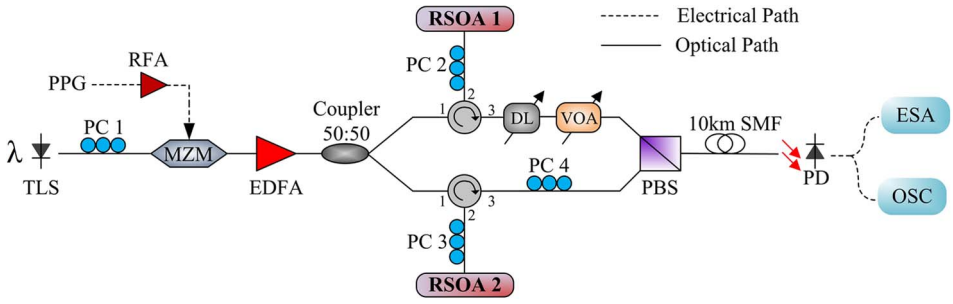

Fig. 2. Experimental setup for high-order UWB signals generation.

(first- and second- order) derivative signals are generated with the input of a specific Gaussian pulse train. It has been shown that high-pass RF filter can be realized by the gain saturation effect in semiconductor optical amplifier (SOA) [22], [23] and the cut-off frequency Δf is defined as

$$\Delta f \propto \frac{1}{2\pi\tau_c}. \tag{1}$$

In equation (1), the cut-off frequency Δf is inversely proportion to the carrier lifetime τ_c. By increasing the input power and bias current to the RSOA, the gain saturation effect in the RSOA is enhanced with the increased carrier density in the active region. However, carrier lifetime may decrease along with the increased in carrier density, which corresponds to a higher cut-off frequency Δf. RSOA is used in the experiment because the gain saturation effect in an RSOA is more significant than that in an SOA [24]. The polarization states of UWB signals generated by RSOA1 and RSOA2 are adjusted, such that they are orthogonal with each other, i.e., TE and TM polarization [indicate in red and blue respectively in Fig. 1(b)]. Thus, high-order UWB signals can be assembled by polarization overlaying. By combining one TE monocycle UWB signal with another TM monocycle UWB signal, triplet UWB signal is obtained. Furthermore, quadruplet UWB can be generated by using one TE monocycle UWB signal and another TM doublet UWB signal.

The experimental setup of our reconfigurable high-order UWB generation scheme is shown in Fig. 2. A tunable laser source (TLS) at 1552.52 nm and output power of 6 dBm is used as the optical carrier. The MZM is driven by a 10 Gb/s pre-coded electrical signal that is amplified by an RF amplifier. The electrical pre-coded signal has the fixed patterns "10000000 00000000" to represent 1 and "00000000 00000000" to represent 0, resulting in a pulse repetition rate of 625 Mb/s. The pattern is modulated onto the optical carrier and a Gaussian like pulse sequence is resulted. The optical pulse sequence is amplified by an Erbium-doped optical fiber amplifier (EDFA) and is sent to the RSOA-MZI. In the RSOA-MZI, the input signal is divided into two branches (upper and lower branches) by a 50 : 50 optical coupler. By adjusting the polarization controllers and the injection of the optical pulse sequences, the output polarization state of both RSOA1 and RSOA2 are stabilized in the TE state. Through adjusting the polarization controller after RSOA2 in the lower branch, the output polarization state of RSOA2 is changed to TM state, which is orthogonal to the upper branch. To eliminate amplitude fluctuation resulting from beating effect between signals of the same wavelength, we use a polarization beam splitter (PBS) to orthogonally overlay the TE signal and TM signal from RSOA-MZI structure. Power and time delay of the upper branch signal are adjusted by a variable optical attenuator (VOA) and a delay line (DL), respectively, to match with the power and time delay of the lower branch. Meanwhile, by precisely tune the VOA in the upper branch and bias current of RSOA 2 in the lower branch, the power deviation result from polarization angle mismatch between PC 4 and PBS will be compensated. These high-order UWB signals are transmitted through a 10-km standard single mode fiber (SMF) and analyzed by an electrical spectrum analyzer (ESA) and a high-speed oscilloscope (OSC).

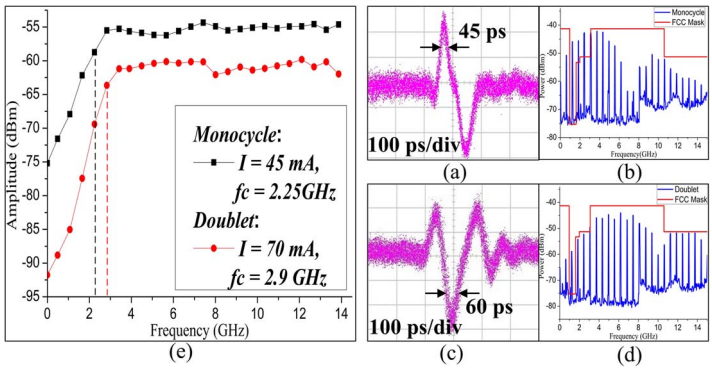

Fig. 3. Frequency response curve of RSOA, waveforms, and spectra of generated monocycle and doublet pulses. Waveforms and spectra of (a) and (b) monocycle UWB signal and (c) and (d) doublet UWB signal.

3. Experimental Results

We analyze the high-pass filtering performance of a single RSOA by measuring the frequency response curve under different bias currents. Due to the limited carrier recovery time, gain saturation in the RSOA has a significant suppressing effect on photonic microwave signals that have a frequency below Δf. In our experiment, an EDFA is placed in front of the RSOA-MZI to guarantee sufficient power for saturating the RSOA gain. After the 50 : 50 optical coupler, the power launched into the RSOA is 1.3 dBm. The measured frequency response curve of the resultant high-pass filter is shown in Fig. 3(e). With RSOA bias current at 45 mA, the corresponding cut-off frequency is 2.25 GHz. After passing through this high-pass filter, the Gaussian-like optical pulse is converted to monocycle UWB signal, and this high-pass filter is equivalent to first-order derivator. By further increasing the bias current to 70 mA, the cut-off frequency of this high-pass filter is increased to 2.9 GHz and doublet UWB pulse is achieved. So second-order derivative signal is able to be realized with higher bias current. It is worth noting that the carrier density of a single stage RSOA has an upper limit, thus, further increasing the bias current does not increase the cut-off frequency of the high-pass filter, which is at around 2.9 GHz.

Fig. 3 shows the monocycle and doublet UWB signals generated by the high-pass filter based on gain saturation in RSOA. Fig. 3(a) and (b) show the waveform and spectrum of monocycle UWB signal $(\mathrm{I} = 45\ \mathrm{mA})$, respectively. This signal has full width half maximum (FWHM) of 45 ps with central frequency of 3.3 GHz and 10-dB bandwidth of 5.8 GHz, which corresponds to a fractional bandwidth of 176%. Fig. 3(c) and (d) show the waveform and spectrum of doublet UWB signal $(\mathrm{I} = 70\ \mathrm{mA})$, respectively. The FWHM of this signal is 60 ps with central frequency of 5.7 GHz and 10-dB bandwidth of 8.1 GHz, which corresponds to a fractional bandwidth of 140%. Comparing Fig. 3(b) and (d), second derivative UWB signal power at lower frequency region (0 GHz–3 GHz) has been further suppressed. That is to say, with larger bias current, the RSOA has a steeper filtering curve and a better suppression effect in the low frequency region.

Frequency responses of the generated triplet and quadruplet UWB signals based on the RSOA-MZI structure are shown in Fig. 4. With the same amplitude polarity but orthogonal polarization state between the upper and lower branches, a (1, 1) coefficient two tap microwave delay line filter is realized. When generating triplet UWB signals, the time delay difference τ between TE mode signal in the upper branch and TM mode signal in the lower branch is set to 150 ps. As shown in Fig. 4(a), a periodic notch filter is realized with free spectrum range (FSR) of 6.67 GHz. At this time, the bias currents of RSOA1 and RSOA2 are 45 mA and 55 mA respectively. Since RSOAs have high pass filtering effect in parallel structure, low frequency parts ($0 \sim 3$ GHz) of the Gaussian signals are suppressed significantly. Due to the periodic filtering effect, there is a power dip near 3 GHz and the suppression ratio with the GPS band at 1.57542 GHz is around 15 dB. When generating quadruplet UWB signals, the bias current of RSOA1 is increased to 70 mA while bias current of RSOA2

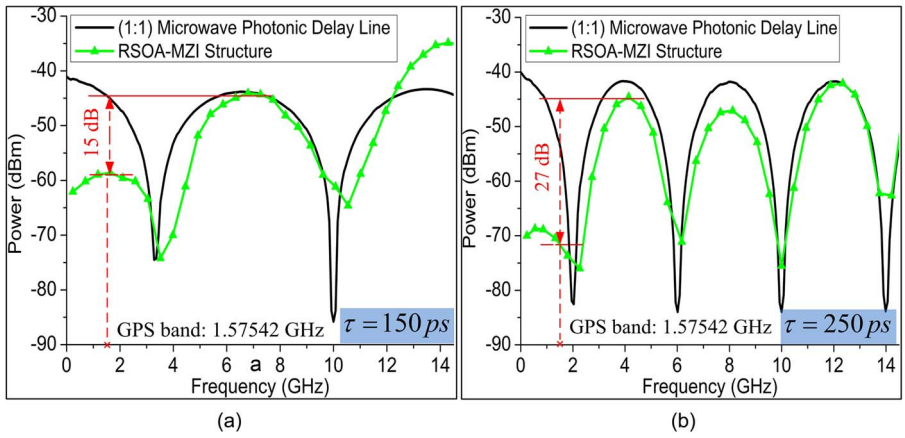

Fig. 4. Frequency response curves of the RSOA-MZI structure. (a) $\tau = 150$ ps. (b) $\tau = 250$ ps.

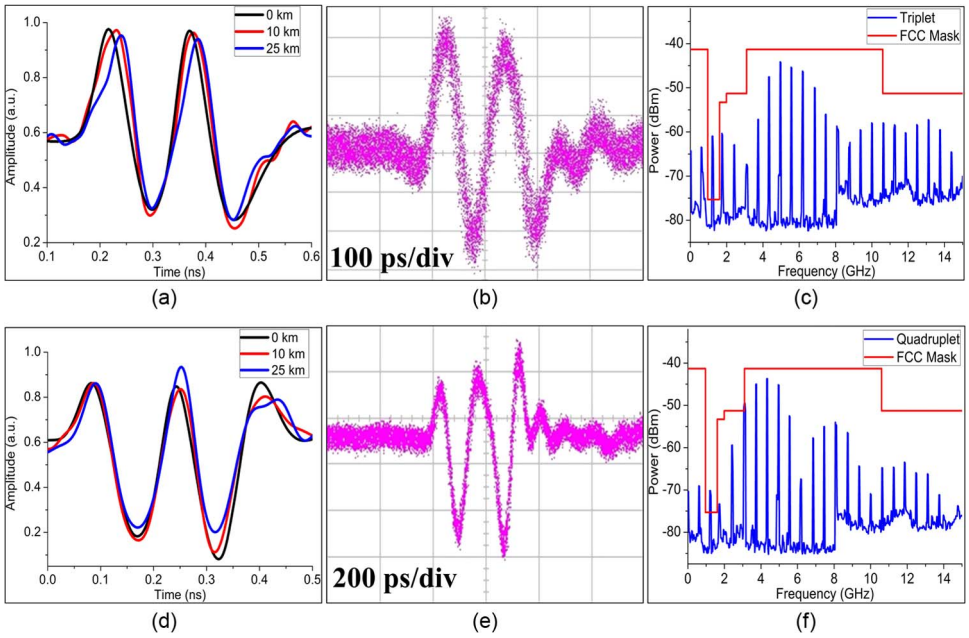

Fig. 5. Simulated and experimental waveforms with spectrums of triplet and quadruplet UWB signals. (a)–(c) Triplet UWB signal, and (d)–(f) Quadruplet UWB signal.

remains the same. The doublet UWB pulses generated by RSOA1 have wider pulse width than a monocycle UWB signal. In order to realize polarization overlaying, the time difference τ in the upper branch is set to 250 ps and a notch filter with FSR of 4 GHz is achieved, as shown in Fig. 4(b). A larger bias current in RSOA corresponds to a decrease in carrier lifetime, while the low frequency filtering effect is enhanced by increasing the bias current of RSOA1. Frequency dip of RSOA-MZI structure is located at 2 GHz with a 27 dB suppression ratio at 1.57542 GHz GPS band.

In order to analyze the influence of fiber chromatic dispersion, we simulate the high-order UWB waveforms under different length fiber transmission. The input signal is optical Gaussian pulse train and the fiber dispersion parameter is set to 16.67 ps/nm·km. The simulation results are shown in Fig. 5(a) and (d). Due to the negative chirp effect in single mode fiber, the leading parts of pulses always propagate faster with longer fiber length. The achieved triplet and quadruplet UWB pulses are all acceptable after 25 km single mode fiber transmission.

Fig. 5(b), (c), (e), and (f) shows the waveforms and spectra of the reconfigurable high-order UWB signals based on parallel RSOAs structure after 10 km single mode fiber transmission. The measured waveform and spectra of the triplet UWB signal are depicted in Fig. 5(b) and (c), respectively. There is a power dip near 3 GHz, where the power level is suppressed to below −60 dBm for 0 GHz to 2 GHz. The central frequency of this triplet UWB signal is located at 4.9 GHz with 10-dB bandwidth of 3.1 GHz, and the corresponding fractional bandwidth is 63.3%. The waveform and spectrum of the quadruplet UWB signal are shown in Fig. 5(e) and (f), respectively. After filtering by the microwave photonic filter, quadruplet UWB signal of central frequency at 4.2 GHz and 10-dB bandwidth of 2.9 GHz is obtained. The fractional bandwidth is 69%. Compared with triplet UWB signal, the generated quadruplet UWB signal has one more amplitude peak in time domain. In frequency domain, especially the 0 GHz to 2 GHz band, the power density of the quadruplet UWB signal is suppressed below −70 dBm. In comparison with the monocycle and doublet UWB signals, the generated triplet and quadruplet UWB signals have less interference with the GPS band.

4. Conclusion

In this paper, a reconfigurable derivative of high-order UWB signals generation scheme is proposed and experimentally demonstrated. Using the RSOA-MZI structure, triplet and quadruplet UWB signals are achieved. The derivative orders can be easily switched by adjusting the RSOA bias currents, time delay and power in the RSOA-MZI structure. With single wavelength operation, all achieved triplet and quadruplet UWB pulses generated are tolerant to fiber dispersion in the UWB over fiber system.

References

[1] Y. Jianping, Z. Fei, and W. Qing, "Photonic generation of ultrawideband signals," *J. Lightw. Technol.*, vol. 25, no. 11, pp. 3219–3235, Nov. 2007.
[2] P. Shilong and Y. Jianping, "A photonic UWB generator reconfigurable for multiple modulation formats," *IEEE Photon. Technol. Lett.*, vol. 21, no. 19, pp. 1381–1383, Oct. 2009.
[3] Q. Wang and J. Yao, "UWB doublet generation using nonlinearly-biased electro-optic intensity modulator," *Electron. Lett.*, vol. 42, no. 22, pp. 1304–1305, Oct. 2006.
[4] Z. Enbo, X. Xing, L. King-Shan, and K. K.-Y. Wong, "A power-efficient ultra-wideband pulse generator based on multiple PM–IM conversions," *IEEE Photon. Technol. Lett.*, vol. 22, no. 14, pp. 1063–1065, Jul. 2010.
[5] Z. Enbo, X. Xing, L. King-Shan, and K. K.-Y. Wong, "High-speed photonic power-efficient ultra-wideband transceiver based on multiple PM–IM conversions," *IEEE Trans. Microw. Theory Tech.*, vol. 58, no. 11, pp. 3344–3351, Nov. 2010.
[6] Y. Dai, J. Du, X. Fu, G. K. P. Lei, and C. Shu, "Ultrawideband monocycle pulse generation based on delayed interference of $\pi/2$ phase-shift keying signal," *Opt. Lett.*, vol. 36, no. 14, pp. 2695–2697, Jul. 2011.
[7] Q. Wang and J. Yao, "Switchable optical UWB monocycle and doublet generation using a reconfigurable photonic microwave delay-line filter," *Opt. Express*, vol. 15, no. 22, pp. 14 667–14 672, Oct. 2007.
[8] M. Bolea, J. Mora, B. Ortega, and J. Capmany, "Optical UWB pulse generator using an N tap microwave photonic filter and phase inversion adaptable to different pulse modulation formats," *Opt. Express*, vol. 17, no. 7, pp. 5023–5032, Mar. 2009.
[9] Q. Wang, F. Zeng, S. Blais, and J. Yao, "Optical ultrawideband monocycle pulse generation based on cross-gain modulation in a semiconductor optical amplifier," *Opt. Lett.*, vol. 31, no. 21, pp. 3083–3085, Nov. 2006.
[10] J. Dong, X. Zhang, J. Xu, D. Huang, S. Fu, and P. Shum, "Ultrawideband monocycle generation using cross-phase modulation in a semiconductor optical amplifier," *Opt. Lett.*, vol. 32, no. 10, pp. 1223–1225, Mar. 2007.
[11] F. Wang, J. Dong, E. Xu, and X. Zhang, "All-optical UWB generation and modulation using SOA-XPM effect and DWDM-based multi-channel frequency discrimination," *Opt. Express*, vol. 18, no. 24, pp. 24 588–24 594, Nov. 2010.
[12] F. Zhang, J. Wu, S. Fu, K. Xu, Y. Li, X. Hong, P. Shum, and J. Lin, "Simultaneous multi-channel CMW-band and MMW-band UWB monocycle pulse generation using FWM effect in a highly nonlinear photonic crystal fiber," *Opt. Express*, vol. 18, no. 15, pp. 15 870–15 875, Jul. 2010.
[13] S. T. Abraha, C. Okonkwo, Y. Hejie, D. Visani, S. Yan, J. Hyun-Do, E. Tangdiongga, and T. Koonen, "Performance evaluation of IR-UWB in short-range fiber communication using linear combination of monocycles," *J. Lightw. Technol.*, vol. 29, no. 8, pp. 1143–1151, Apr. 2011.
[14] X. Fu, Y. Dai, and C. Shu, "Reconfigurable photonic ultrawideband pulse generation from an optically injected semiconductor laser," *Opt. Lett.*, vol. 38, no. 6, pp. 968–970, Mar. 2013.
[15] S. Pan and J. Yao, "Optical generation of polarity- and shape-switchable ultrawideband pulses using a chirped intensity modulator and a first-order asymmetric Mach–Zehnder interferometer," *Opt. Lett.*, vol. 34, no. 9, pp. 1312–1314, Mar. 2009.

[16] L. Pengxiao, C. Hongwei, W. Xu, Y. Hongchen, C. Minghua, and X. Shizhong, "Photonic generation and transmission of 2-Gbit/s power-efficient IR-UWB signals employing an electro-optic phase modulator," *IEEE Photon. Technol. Lett.*, vol. 25, no. 2, pp. 144–146, Jan. 2013.
[17] E. Wong, L. Ka Lun, and T. B. Anderson, "Directly modulated self-seeding reflective semiconductor optical amplifiers as colorless transmitters in wavelength division multiplexed passive optical networks," *J. Lightw. Technol.*, vol. 25, no. 1, pp. 67–74, Jan. 2007.
[18] K. Y. Cho, Y. Takushima, and Y. C. Chung, "10-Gb/s Operation of RSOA for WDM PON," *IEEE Photon. Technol. Lett.*, vol. 20, no. 18, pp. 1533–1535, Sep. 2008.
[19] G. Chen and S. Pan, "Photonic generation of ultrawideband signals based on frequency-dependent gain saturation in a reflective semiconductor optical amplifier," *Opt. Lett.*, vol. 37, no. 20, pp. 4251–4253, Oct. 2012.
[20] Z. Weiwei, J. Sun, W. Jian, C. Cheng, and Z. Xinliang, "Ultra-wideband pulse train generation based on turbo-switch structures," *IEEE Photon. Technol. Lett.*, vol. 21, no. 5, pp. 271–273, Mar. 2009.
[21] K. Youngbok, J. Sie-Wook, C. Yong-Kyu, and P. Chang-Soo, "UWB triplet pulse generation based on gain switching of RSOA," in *Proc. PGC*, 2010, pp. 1–2.
[22] K. Sato and H. Toba, "Reduction of mode partition noise by using semiconductor optical amplifiers," in *Proc. IEEE 17th Int. Semicon. Laser Conf., Conf. Dig.*, 2000, pp. 73–74.
[23] R. Boula-Picard, M. Alouini, J. Lopez, N. Vodjdani, and J. C. Simon, "Impact of the gain saturation dynamics in semiconductor optical amplifiers on the characteristics of an analog optical link," *J. Lightw. Technol.*, vol. 23, no. 8, pp. 2420–2426, Aug. 2005.
[24] J. M. Kang, T. Y. Kim, I. H. Choi, S. H. Lee, and S. K. Han, "Self-seeded reflective semiconductor optical amplifier based optical transmitter for up-stream WDM-PON link," *IET Optoelectron.*, vol. 1, no. 2, pp. 71–81, 2007.